

See discussions, stats, and author profiles for this publication at: <https://www.researchgate.net/publication/273720609>

Multi-SunSynchronous Orbits in the Solar System

Article in *Earth Moon and Planets* · May 2014

DOI: 10.1007/s11038-014-9432-z

CITATIONS

8

READS

396

4 authors, including:



Carlo Olivieri

Sapienza University of Rome

52 PUBLICATIONS 628 CITATIONS

[SEE PROFILE](#)



Marco Cinelli

National Institute of Astrophysics

19 PUBLICATIONS 160 CITATIONS

[SEE PROFILE](#)



Christian Circi

Sapienza University of Rome

104 PUBLICATIONS 1,095 CITATIONS

[SEE PROFILE](#)

Some of the authors of this publication are also working on these related projects:



Observation of Europa [View project](#)



Dynamical problem of the hopping rover with unilateral constraint by considering the asteroid complex terrain [View project](#)

Multi-SunSynchronous Orbits in the Solar System

Emiliano Ortore · Christian Circi · Carlo Ulivieri · Marco Cinelli

Received: 10 October 2013 / Accepted: 30 March 2014 / Published online: 5 April 2014
© Springer Science+Business Media Dordrecht 2014

Abstract Performances of a planetary observation system are strongly related to the choice of the orbit used. Trajectories with characteristics of periodicity are very useful for the assessment of time-varying phenomena and thus Periodic SunSynchronous and Periodic Multi-SunSynchronous Orbits are particularly suitable to this end. In this paper, the research into these kinds of orbits, previously proposed for the Earth and Mars, has been extended to planets of the Solar System and to their principal moons. In general, these trajectories are typically obtained under the hypothesis that the J_2 harmonic is predominant with respect to the other orbital perturbations, since this allows an analytical solution. However, the hypothesis of J_2 predominant is not always verified in the Solar System and so analytical techniques must be replaced by numerical simulations. Interesting results have been obtained for the planets Mars and Jupiter and for the moons Europa, Callisto and Titan, where periodic trajectories with reduced revisit times and low altitudes have been found. These solutions allow the observation of time-varying phenomena with high spatial and temporal resolution.

Keywords Multi-SunSynchronous Orbits · Periodic orbits · Planetary observation

E. Ortore (✉) · C. Circi · C. Ulivieri · M. Cinelli
Department of Astronautical, Electrical and Energetic Engineering, Sapienza University of Rome, Via
Salaria, 851-881, 00138 Rome, Italy
e-mail: emiliano.ortore@uniroma1.it

C. Circi
e-mail: christian.circi@uniroma1.it

C. Ulivieri
e-mail: carlo.ulivieri@uniroma1.it

M. Cinelli
e-mail: cinelli.marco@virgilio.it

1 Introduction

The observation of celestial bodies is fundamental to understand in depth the history and the evolution of the Solar System and the space agencies take in due consideration the missions aimed at analysing the planets and their moons. For example, the Jupiter icy moons explorer mission (JUICE), which is the first Large-class mission in ESA's Cosmic Vision 2015–2025 programme, will spend at least 3 years making detailed observations of the biggest planets in the Solar System and three of its largest moons: Ganymede, Callisto and Europa (<http://sci.esa.int/science-e/www/object/index.cfm?fobjectid=51417>).

In the planetary observation field, the choice of the trajectory to be described around the celestial bodies undoubtedly represents a factor of key importance and several solutions can be exploited to retrieve remotely sensed information about the atmosphere and the surface of a celestial body (Liu et al. 2010). Novel orbits around Mars, Mercury and Venus have recently been proposed to enhance the opportunities for remote sensing of these planets by using low-thrust propulsion systems (Anderson et al. 2013). Other important examples are represented by the repeating ground track orbits (periodic orbits), the Sun-Synchronous Orbit (SSO), the stationary orbits (Liu et al. 2012; Wytryszczak 1998), the frozen orbits (Coffey et al. 1994; Aorpimai and Palmer 2003; Liu et al. 2011a), the orbits at critical inclination (Coffey et al. 1986; Liu et al. 2011b) and the multi-stationary orbits (Ortore and Olivieri 2008; Ortore et al. 2011). In particular, the Periodic SunSynchronous Orbits (PSSOs), which merge the repeating ground track and sunsynchronism conditions, produce cyclic observations of a given area at the same local time. This characteristic allows the minimization of the spectral signature variations of the observed area due to the different positions of the Sun. However, if on one hand this typology of orbits provides the optimal condition to appreciate the variations of the characteristics of a given target, on the other hand it does not permit a temporal analysis of the phenomena characterized by typical diurnal variations (surface temperature, atmospheric density, aerosol concentration, etc....) (Capderou and Forget 2004; Ortore et al. 2013). An estimate of these phenomena can be optimally carried out by using the so-called Periodic Multi-SunSynchronous Orbits (PMSSOs). In fact, with such orbits, a given region of a celestial body is periodically observed in solar illumination conditions that follow a regular cycle (Ortore et al. 2012).

Both the PSSOs and PMSSOs find a direct realization around celestial bodies in which the planetary oblateness is predominant with respect to the other harmonics of the gravitational field and to the third-body perturbations. The PMSSOs have recently been investigated for the Earth and Mars and both circular and elliptical solutions have been proposed. The effects of the higher harmonics of the gravitational fields (more marked for Mars) have led to the introduction of corrective factors, depending on the orbital altitude and inclination, which avoid corrective manoeuvres (Ortore et al. 2012; Circi et al. 2012).

In this paper, the analysis is extended to planets and natural moons of the Solar System, also taking into account the cases of non predominant J_2 celestial bodies (planetary oblateness is of the same order of magnitude as the higher gravitational harmonics and/or as the third-body perturbation). In these cases, the investigation can be carried out only by means of numerical solutions. The paper is organised as follows: in Sect. 2 the concept of multi-sunsynchronism is presented, for both predominant and non predominant J_2 cases; in Sect. 3 the feasibility of obtaining circular PSSOs and PMSSOs around all the planets of the Solar System is analysed; in Sect. 4 the same investigation is performed around the principal moons of Jupiter and Saturn; finally, in Sect. 5, solutions for Europa, Callisto and Titan are illustrated and proposed.

2 The Multi-SunSynchronism Concept

As known, PSSOs allow cyclic observations of a planet in which a given area is periodically observed at the same local time. These orbits are identified by two relationships, representing respectively the ground track periodicity and the sunsynchronism condition:

$$mD_n = RT_n \quad (1)$$

$$\dot{\Omega} = \dot{\Omega}_s \quad (2)$$

where D_n is the nodal day, m is the integer number of nodal days between two successive passes over the same ground track, R is the integer number of orbits accomplished in m nodal days (R and m are prime numbers one to the other), T_n is the nodal period, $\dot{\Omega}$ is the temporal variation of the Right Ascension of the Ascending Node (RAAN = Ω) and $\dot{\Omega}_s$ is the apparent mean angular motion of the Sun in a non-rotating reference frame centred at the planet's centre. Representing the curves coming from Eqs. (1) and (2) in the plane (i , a), where i is the orbit inclination and a the semi-major axis of the orbit, the intersections of curves (1), plotted for different values of the ratio R/m (number of orbits per nodal day), and (2), provide the finite number of PSSO solutions.

The repeated observation of a region at different local times can instead be carried out by considering the PMSSOs. The system of equations which identify this typology of orbit is composed of three equations. In fact, to the periodicity condition (1), the following Eqs. (3) and (4) have to be added:

$$mD_n = RT_n \quad (1)$$

$$nD_n = \frac{2\pi}{|\dot{\Omega} - \dot{\Omega}_s|} \quad (3)$$

$$n = I \cdot m \quad (4)$$

where n is the integer number of nodal days after which the same local time of observation occurs and I is an integer number. Eq. (3) provides the periodicity condition in the solar illumination (multi-sunsynchronism condition). In fact, every n nodal days the angle between the line Sun-planet and the nodal line of the orbit re-assumes the same value and it can be obtained by means of direct or retrograde orbits: when $i < 90^\circ$ the line Sun-planet and the nodal line move in opposite directions, whereas if $i > 90^\circ$ they move in the same direction. Moreover, due to the presence of the absolute value in Eq. (3), for each value of n a pair of solutions occurs, one for $\dot{\Omega} > \dot{\Omega}_s$, the other one for $\dot{\Omega} < \dot{\Omega}_s$. Eq. (4) allows the realization of orbits in which the periodicity of the illumination conditions is multiple of the ground track periodicity. Then, a given area is observed I times in n nodal days (at a regular interval of m nodal days) and the local time temporal sampling is given by the ratio D_S/I , where D_S is the solar day:

$$D_S = \frac{2\pi}{\omega_P - \dot{\Omega}_s} \quad (5)$$

where ω_P is the angular velocity of the planet around its rotation axis. In other words, the observations of an area occur in succession at a local time that varies according to the following law: initial local time + $(ND_S)/I$ (where $N = 1, 2, \dots, I$) and, at the end of the n days, the initial local time is re-obtained.

It is important to note that by replacing Eq. (2) in (3), the value of n tends to be infinite. This means that the PSSO condition can be considered as a particular PMSSO case, in which the same solar illumination conditions are obtained at every pass. In this case the line Sun-planet and the nodal line move in the same direction (the orbits can only be retrograde) and the angle between them is constant (SSO condition).

In the cases of J_2 predominant, the nodal day and period can be expressed in the following approximate forms:

$$D_n \cong \frac{2\pi}{\omega_P - \dot{\Omega}_{J_2}} \quad (6)$$

$$T_n \cong \frac{2\pi}{\dot{\omega}_{J_2} + \dot{M}_{J_2} + \sqrt{\frac{\mu_P}{a^3}}} \quad (7)$$

where $\dot{\omega}_{J_2}$ and \dot{M}_{J_2} are respectively the temporal variations of the argument of pericentre ω and the mean anomaly M due to the harmonic J_2 (the subscript J_2 indicates that the variation of the parameter only refers to the J_2 contribution), while $\sqrt{\frac{\mu_P}{a^3}}$ is the mean motion of the probe orbiting around the celestial body (μ_P is the gravitational constant of the celestial body). As known, for a SSO, $D_n = D_S$. In the J_2 predominant cases, introducing in Eqs. (6) and (7) the expressions of the temporal variations of Ω , ω and M (R_P = equatorial mean radius of the celestial body, e = orbit eccentricity, i = orbit inclination):

$$\dot{\Omega}_{J_2} = -\frac{3}{2}J_2 \frac{R_P^2}{a^{7/2}(1-e^2)^2} \sqrt{\mu_P} \cos i \quad (8)$$

$$\dot{\omega}_{J_2} = \frac{3}{2}J_2 \frac{R_P^2}{a^{7/2}(1-e^2)^2} \sqrt{\mu_P} \left(2 - \frac{5}{2} \sin^2 i\right) \quad (9)$$

$$\dot{M}_{J_2} = \sqrt{\frac{\mu_P}{a^3}} + \frac{3}{2}J_2 \frac{R_P^2}{a^{7/2}(1-e^2)^{3/2}} \sqrt{\mu_P} \left(1 - \frac{3}{2} \sin^2 i\right) \quad (10)$$

the PSSO and PMSSO solutions can be retrieved in an analytical way. These solutions are obtained solving respectively the systems of Eqs. (1), (2) and (1), (3), (4). In particular, for circular orbits, it is $e = 0$ and the position of the probe is identified by the argument of latitude, which is the sum of argument of pericentre and mean anomaly (not singularly defined).

In the non predominant J_2 cases, the nodal day and period expressions are general:

$$D_n = \frac{2\pi}{\omega_P - \dot{\Omega}} \quad (11)$$

$$T_n = \frac{2\pi}{\dot{\omega} + \dot{M} + \sqrt{\frac{\mu_P}{a^3}}} \quad (12)$$

and the variations of the orbit elements are also due to other perturbations. Therefore, in these cases, the PSSO and PMSSO solutions ought to be numerically obtained by solving the above mentioned systems of equations. To this purpose, it is important to remark that solutions can be retrieved if the temporal trends $\dot{\Omega}$, $\dot{\omega}$, \dot{M} are (at least) quasi-linear. In fact, in this case, the nodal period and day [Eqs. (11) and (12)] can be considered as constants with a satisfactory approximation.

3 Planets of the Solar System

With reference to the planets of the Solar System, the possible applications of the introduced trajectories have been investigated.

As far as the Earth and Mars are concerned, the possibility of retrieving PMSSOs has been investigated in (Ortore et al. 2012; Circi et al. 2012) and several solutions have been proposed for the observation of these planets. While the PSSO solutions around the Earth are well-known and have extensively been used for decades for the remote sensing of our environment (since the early LANDSAT and SPOT satellites), the PSSOs around Mars would represent innovative solutions. For this reason, the possibility of obtaining this typology of orbit has been investigated here. Table 1 shows PSSO solutions obtained at low altitude (h) around Mars, considering only the J_2 perturbation ($J_2 = 1.955454 \times 10^{-3}$) and a revisit time from 1 to 10 nodal days.

The relatively high eccentricity (0.2056) of Mercury's orbit around the Sun prevents the realization of both sunsynchronism and multi-sunsynchronism conditions (without using propulsive systems). This eccentricity produces indeed significant differences between the angular velocity of the planet and its mean value ($\dot{\Omega}_S$), reaching a maximum variation of 41.24 %, which prevents the consideration of a constant value for this parameter (without introducing significant errors in the solar illumination conditions of observation). In addition, the long duration of the nodal day would lead to the realization of repeating ground track orbits (and consequently of PMSSOs) with excessively long cycles of observation.

Numerical simulations for Venus, which is a case of non predominant J_2 , carried out using the model with 20×20 (order and degree) harmonics described in (Konopliv et al. 1999), have shown that the gravitational perturbations due to the planetary asymmetry do not allow the realization of the condition (2). Moreover, similar to the Mercury case, the realization of repeating ground track orbits would be significantly limited by the very long duration of the nodal day.

As for the outer planets, only the Jupiter case has been analysed. In fact, for Saturn, Uranus and Neptune (which, like Jupiter, are planets at J_2 predominant), the long distance from the Sun is such as to make non optimal the use of both the proposed orbit typologies, even though the limited duration of their nodal days (about respectively 10.6, 17.2 and 16.1 h) would allow reduced revisit periods of an area of interest.

Jupiter is characterized by a high value of J_2 (1.469643×10^{-2}) and therefore the sunsynchronism condition may be obtained, at a relatively low altitude, only with quasi-polar orbits. Figure 1 shows PSSO solutions around Jupiter as points belonging to the inclination-altitude sun-synchronism curve (intersections of the curves given by Eqs. (1) and (2), with $\dot{\Omega}_S = 0.0831^\circ/\text{day}$), considering only the planetary oblateness.

However, for the solutions of Fig. 1, it is important to remark that the highest altitudes fall within Jupiter's intense radiation belts, limiting the probe operational life-time.

Table 2 shows the revisit times (m) and the number of revolutions (R) for the solutions of Fig. 1.

Always considering only the J_2 perturbation, an investigation into the PMSSO solutions for Jupiter has also been executed. Figure 2 shows PMSSO solutions, considering h as a function of i and n up to 50. As mentioned before, for a single value of n a pair of solutions occurs, one for $\dot{\Omega} > \dot{\Omega}_S$ (left part of the figure), the other one for $\dot{\Omega} < \dot{\Omega}_S$ (right part of the figure). In both cases, for a given value of inclination, the altitude increases with increasing values of n .

Table 1 PSSO solutions around Mars

Solution	h (km)	i (°)	m	R
1	523.52	93.27	1	12
2	755.32	94.00	1	11
3	419.45	92.97	2	25
4	453.50	93.07	3	37
5	597.08	93.49	3	35
6	674.25	93.73	3	34
7	369.94	92.84	4	51
8	470.59	93.12	4	49
9	694.36	93.80	4	45
10	399.54	92.92	5	63
11	567.40	93.40	5	59
12	658.60	93.68	5	57
13	706.31	93.83	5	56
14	488.20	93.17	6	73
15	560.06	93.38	6	71
16	349.36	92.79	7	90
17	434.03	93.01	7	87
18	554.70	93.36	7	83
19	720.29	93.88	7	78
20	345.91	92.78	8	103
21	496.93	93.19	8	97
22	724.52	93.89	8	89
23	343.21	92.77	9	116
24	430.76	93.01	9	112
25	727.84	93.91	9	100
26	379.75	92.87	10	127
27	460.29	93.09	10	123
28	682.32	93.76	10	113

With respect to the Earth and Mars's cases (Ortore et al. 2012; Circi et al. 2012), solutions with lower values of n have been retrieved. Thanks to the limited duration of the nodal day (about 10 h), these reduced values of n lead to the possibility of obtaining low altitude PMSSOs. For example, taking into consideration the values of $n = 20$ and $i = 40^\circ$, the corresponding altitude of the orbit would be about 1,000 km. These solutions would be useful to track gross atmospheric features, such as long-lived storms and wave patterns in atmospheric jets. In particular, if the probe observes in the mid to far infrared wavelengths, where the instrument detects upwelling thermal energy on both the day and night sides of the planet, the observations could be made in both the ascending and descending parts of the orbit. However, also for the solutions of Fig. 2, the highest altitudes fall within Jupiter's intense radiation belts, limiting the probe operational life-time.

At the same time, the observation of Jupiter's moons may significantly take advantage of the aforesaid typologies of orbits. For such a reason, this matter will be investigated in Sect. 4.

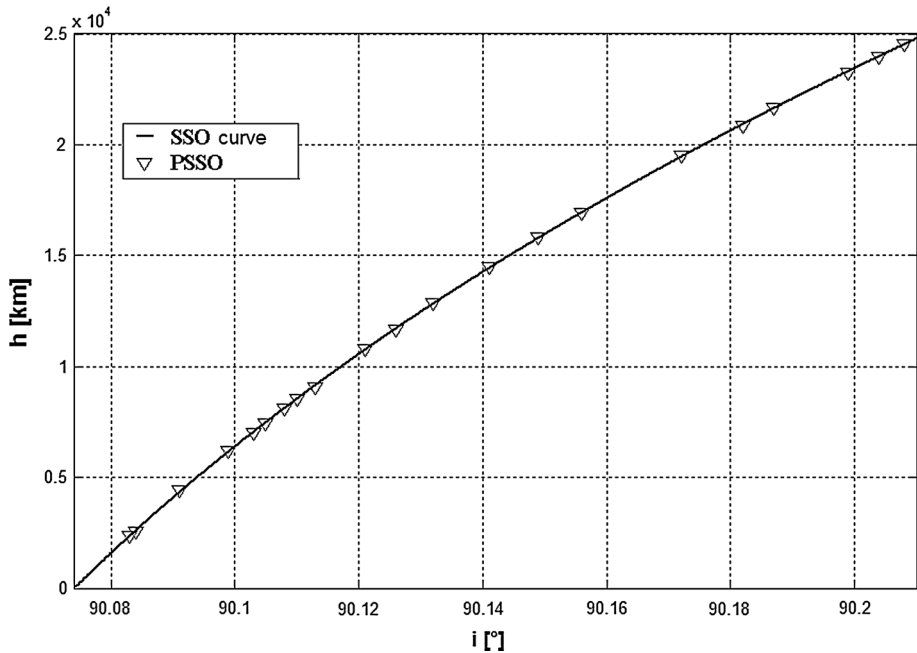


Fig. 1 PSSO solutions around Jupiter

Although the case of Saturn has been excluded from this study because of its great distance from the Sun, its natural satellite Titan, for its great scientific interest, will also be taken into consideration in Sect. 4.

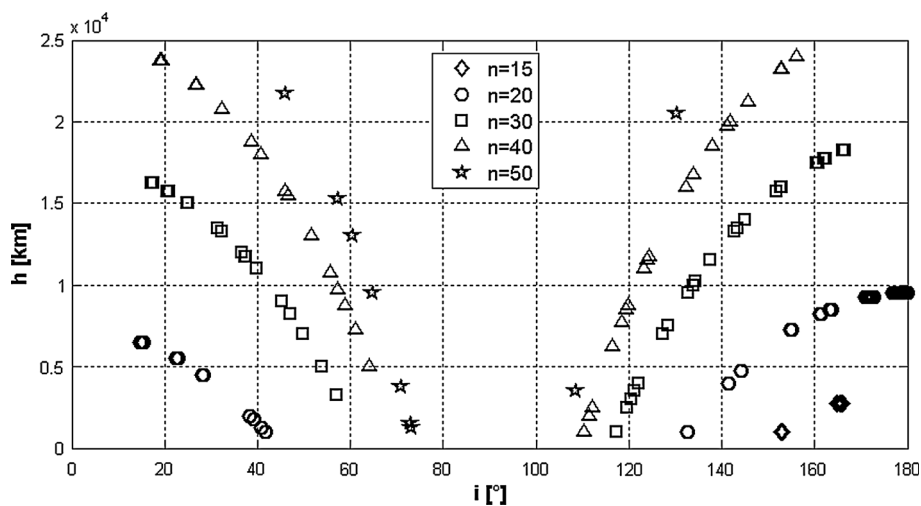
4 Titan and the Main Moons of Jupiter

Among all the moons of the Solar System, the principal moons of Jupiter and Saturn (Io, Europa, Ganymede, Callisto and Titan) undoubtedly represent the cases of major interest for the realization of the proposed orbits. Since, for these moons, it is not possible to consider the hypothesis of J_2 predominant, the feasibility of obtaining PSSOs and PMSSOs around these celestial bodies ought to be investigated following a numerical approach. In addition, due to the gravitational influence of the planet around which the moons are orbiting, the third-body effects must also be taken into account in the numerical simulations. In all these cases, as a value of $\dot{\Omega}_S$, the value of the corresponding planet has been assumed as a reference, neglecting the variation α due to the moon's motion around the planet (Fig. 3). In fact, the maximum oscillations of the lines Sun-moon with respect to the Sun-planet line, reported in Table 3, are all small enough to be neglected (for Saturn it is $\dot{\Omega}_S = 0.0335^\circ/\text{day}$).

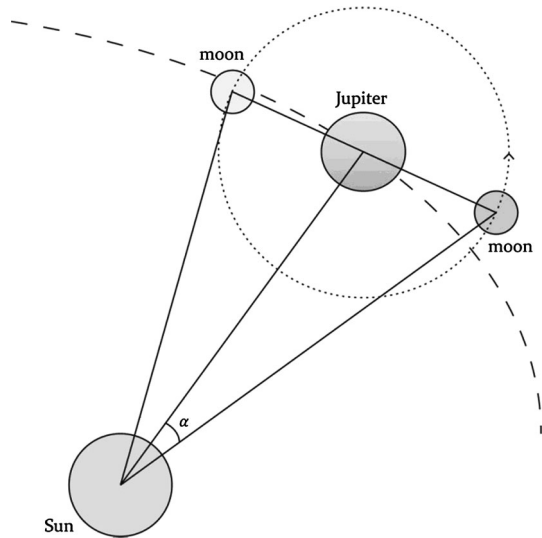
Due to the nearness of Io to Jupiter (about 421,700 km) and to Europa and Ganymede, the orbits around Io are strongly perturbed. For this reason, the repeating ground track condition (Eq. (1)) around this natural satellite cannot be satisfied. Moreover, numerical simulations, performed using the gravitational model (Anderson et al. 2001a), which takes the J_2 , J_{22} , J_3 and J_4 harmonics into account, have also shown that the sun-synchronism condition is unachievable, always resulting $\dot{\Omega} > \dot{\Omega}_S$.

Table 2 PSSO solutions around Jupiter

h (km)	i (°)	m	R
4,439.05	90.09	1	3
14,494.09	90.14	2	5
10,798.07	90.12	3	8
9,088.02	90.11	4	11
20,871.85	90.18	4	9
8,104.19	90.11	5	14
16,912.08	90.16	5	12
7,463.29	90.11	6	17
23,266.53	90.20	6	13
7,014.88	90.10	7	20
12,860.35	90.13	7	18
23,978.17	90.20	7	15
2,347.50	90.08	8	25
11,684.09	90.13	8	21
24,521.47	90.21	8	17
2,572.97	90.08	9	28
8,537.56	90.11	9	25
15,817.00	90.15	9	22
21,654.06	90.19	9	20
6,219.43	90.10	10	29
19,505.49	90.17	10	23

**Fig. 2** PMSSO solutions around Jupiter

As for Europa, the gravitational model (Anderson et al. 1998), which considers the J_2 , J_{22} , J_3 and J_4 harmonics, has been taken into consideration. The results have shown that, when $\dot{\Omega} = \dot{\Omega}_s$, the third-body effects cause orbital variations which determine the collision

Fig. 3 Variation of the line Sun–moon**Table 3** Maximum oscillation of the lines Sun–moon for natural satellites of Jupiter and Saturn

	Io	Europa	Ganymede	Callisto	Titan
α_{MAX}	0.0310°	0.0494°	0.0788°	0.1386°	0.0491°

of the orbiting probe with the moon in reduced times. In (Lara and Russell 2007) an investigation into the life-times has been carried out taking into consideration families of periodic orbits with different inclinations. In particular, orbits for scientific missions having inclination between 70° and 110° and altitude of approximately 100 km allows life-times of about 110 days. In order to obtain long times before this collision, values of inclination lower than 45° have to be taken into account. In this paper, PSSO and PMSSO solutions around Europa have been determined and their description will be provided in Sect. 5.

For Ganymede, the model (Anderson et al. 1996), which takes J_2 , J_{22} , J_3 and J_4 into account, has been considered. The SSO condition at low altitude (400 km) is verified in the inclination range $93^\circ < i < 94^\circ$ where, although the distance of this moon from Jupiter is about 1,070,000 km, the third-body effects cause short life-times (collision probe–moon). As for the PMSSOs, very high values of n have been obtained, which lead to excessively long cycles of observation.

For Callisto, the model (Anderson et al. 2001b), which also considers J_2 , J_{22} , J_3 and J_4 , has been used. The great distance from Jupiter reduces the perturbative effects making the SSO condition possible at low altitude, with inclinations lower than 112° . Similar to the Ganymede case, as for the PMSSOs, excessively high values of n have been retrieved. The PSSO solutions will be described in Sect. 5.

Finally, for Titan, the model with 3×3 (order and degree) harmonics described in (Iess et al. 2010) has been taken into consideration. The results have shown that PSSO solutions are possible in the range of altitude going from 1,400 to 1,500 km (the corresponding inclination interval is $101.2\text{--}101.9^\circ$). Lower altitudes have been excluded due to the strong effects of the atmospheric drag. On the other hand, the employment of PMSSOs is strongly

limited because of the high values of the nodal day (16 terrestrial days) and n (the minimum value is 40). The PSSO solutions will also be described in Sect. 5.

In conclusion, Table 4 summarizes the results obtained for the principal moons of Jupiter and Saturn on the feasibility of obtaining PSSOs and PMSSOs.

5 Solutions Around Europa, Callisto and Titan

According to Table 4, PSSO and PMSSO solutions around Europa (Sect. 5.1), PSSO solutions around Callisto (Sect. 5.2) and around Titan (Sect. 5.3) have been investigated.

5.1 Europa

In this case the hypothesis $\dot{\Omega} \cong \text{constant}$ is well verified. As an example, Fig. 4 shows the (quasi-linear) Ω trend as a function of time, considering a semi-major axis of 1,726.93 km and an inclination of 43.70°.

Table 5 shows PSSO solutions. Note that only the values of inclination close to 93° allow Eq. (2) to be satisfied and that after about 30 terrestrial days the periodicity condition [Eq. (1)] is no longer exactly verified.

As mentioned in Sect. 4, only the orbits with an inclination $< 45^\circ$ guarantee long collision times. Since the investigation of time-varying phenomena require repeated cycles of observation, for the PMSSOs values of $i < 45^\circ$ have been taken into consideration. Table 6 shows PMSSO solutions.

These orbits make the observation of mid-low latitudes of Europa in multi-sun-synchromism conditions with reduced revisit times ($m = 1$ or 2) possible. As said, the parameter I represents the number of observations (performed in different solar illumination conditions) occurring in n nodal days at regular intervals of m nodal days. Since two subsequent observations are characterized by a local time phasing of D_S/I , high temporal samplings are obtained. Table 7 reports the local time phasing between one observation and the next over the same area.

Thanks to high temporal samplings, all the proposed solutions would allow a deep analysis of the temporal evolution of physical and chemical characteristics of the atmosphere and of the surface of Europa. In particular, among the retrieved solutions, number 4 presents the following additional advantages:

- higher inclination (43.70°), which allows a greater latitude coverage;
- lower altitude (161.93 km), which leads to a better ground spatial resolution;
- smaller minimum track distance (131.11 km), which limits the sensor swath needed to achieve a complete longitudinal coverage of the moon.

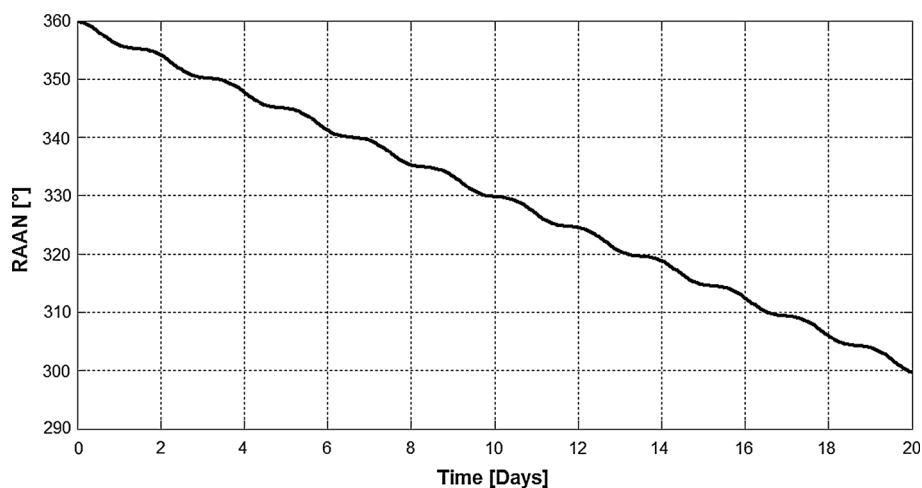
Then, numerical simulations have been carried out to investigate the perturbative effects on this solution. The results have shown weak variations of the orbit elements:

- the semi-major axis oscillates by 2 km around a mean value of 1,724.86 km;
- the eccentricity always remains below the value 0.003;
- the inclination oscillates with an amplitude of 3°.

These variations produce limited displacements of the ground track pattern with respect to the nominal configuration (Table 8).

Table 4 Possibility of gaining PSSOs and PMSSOs around the moons of Jupiter and Saturn

Type of orbit	Io	Europa	Ganymede	Callisto	Titan
PSSO	No	Yes	No	Yes	Yes
PMSSO	No	Yes	No	No	No

**Fig. 4** RAAN variation for an orbit of semi-major axis 1,726.93 km and inclination 43.70° around Europa**Table 5** PSSO solutions around Europa

h (km)	i (°)	m	R	T _n (h)
99.35	92.90	5	204	2.0906
107.65	92.89	2	81	2.1061
150.24	92.93	1	39	2.1871
200.97	92.95	3	112	2.2848
252.89	92.98	4	143	2.3860
296.57	93.00	2	69	2.4724

Table 6 PMSSO solutions around Europa with $i < 45^\circ$

Solution	h (km)	i (°)	D _n (terrestrial day)	T _n (h)	m	R	n (nodal day)	I	S _m (km)
1	170.20	25.00	3.4272	2.2230	1	37	28	28	265.76
2	191.20	37.85	3.4430	2.2639	2	73	32	16	134.70
3	177.48	42.95	3.4496	2.2376	1	37	34	34	265.76
4	161.93	43.70	3.4496	2.2077	2	75	34	17	131.11

Table 7 Local time phasing for the solutions of Table 6

Solution	D _S /I (h)
1	2.9376
2	5.1645
3	2.4350
4	4.8700

The results demonstrate that the displacement is periodic and limited to within about 20 km.

Also for the temporal displacements with respect to the nominal passes, reduced values have been obtained (Table 9).

In fact, after 2,111 days, the accumulated delay reaches the value of only 6 min.

In conclusion, the reduced perturbative effects obtained for Solution 4 would allow the exploitation of this solution without the necessity of introducing manoeuvres to correct the orbit elements during the mission. Moreover, a broad range of numerical simulations has also been executed to examine the behaviour of the other solutions of Table 6 and the results have led to the same conclusion.

5.2 Callisto

By means numerical simulations PSSOs around Callisto have also been investigated. Table 10 shows the selected solutions, which are characterized by low altitudes (from 189.46 to 356.57 km), with corresponding inclination values from 110.01 to 111.49°, revisit times (m) from 1 to 7 nodal days (equal to 117 terrestrial days) and very small distances between adjacent ground tracks (the maximum value of S_m is 108.95 km).

In general, the choice between the different proposed solutions depends on the mission requirements (mainly spatial coverage, resolution and periodicity of observation).

As an example, Solution 2 of Table 10 has been analysed in terms of orbital perturbations and the results have shown that:

- the semi-major axis is subject to negligible variations;
- the eccentricity is subject to significant variations (Fig. 5);
- the orbit inclination is subject to a variations of 0.4°.

The figure highlights how for the first 3 years the eccentricity variation remains limited, reaching a value of about 0.005 (the corresponding altitude difference between apocentre and pericentre is 25 km). Such a solution would lead to an impact with Callisto after 4 years (which can be considered sufficient time to observe the moon). If a longer period is requested, appropriate corrective manoeuvres have to be introduced. Considering a lifetime of 6 years, an analysis has been carried out to establish the optimal manoeuvre strategy and Fig. 6 reports the obtained results for the eccentricity correction, in terms of total ΔV as a function of the number of manoeuvres. The optimal strategy is characterized by a total of 9 manoeuvres (one manoeuvre every 235 days). Each manoeuvre requires a velocity variation of 0.35 m/s (to be provided in the perpendicular direction to the velocity of the probe) for a total ΔV of 3.15 m/s.

However, also the other strategies present limited consumptions.

Table 8 Displacements from the nominal track for Solution 4

Terrestrial day	Equatorial distance from the nominal ground track (km)
6.899	2.4
20.697	4.7
34.496	2.1
48.294	5.1
62.092	13.9
75.890	20.6
89.689	22.5
103.487	19.2
117.285	13.5

Table 9 Delays from the nominal passes for Solution 4

Terrestrial day	Delay time from the nominal pass (min)
117.285	0.10
351.855	0.40
586.425	0.87
820.996	1.25
1,055.566	1.90
1,290.136	2.60
1,524.706	3.50
1,759.276	4.48
1,993.847	5.55

Table 10 PSSO solutions around Callisto

Solution	h (km)	i (°)	T _n (h)	R	m	S _m (km)
1	291.64	110.95	2.893	139	1	108.95
2	198.65	110.10	2.745	293	2	51.69
3	259.77	110.67	2.842	283	2	53.51
4	338.08	111.34	2.967	271	2	55.88
5	220.58	110.31	2.779	434	3	34.89
6	322.34	111.21	2.942	410	3	36.94
7	308.04	111.09	2.919	551	4	27.49
8	206.92	110.18	2.758	729	5	20.77
9	231.26	110.41	2.796	719	5	21.06
10	325.95	111.24	2.948	682	5	22.21
11	243.19	110.52	2.815	857	6	17.67
12	293.97	110.97	2.896	833	6	18.18
13	189.46	110.01	2.730	1,031	7	14.69
14	226.97	110.37	2.789	1,009	7	15.01
15	356.57	111.49	2.997	939	7	16.13

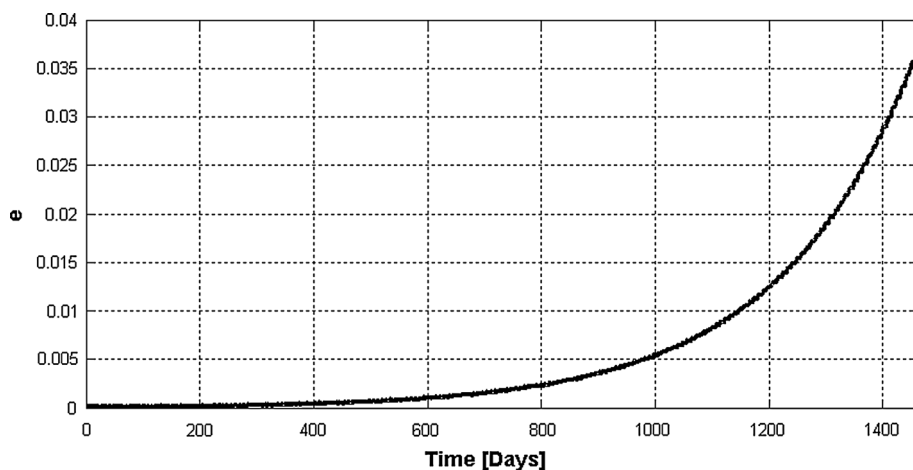


Fig. 5 Eccentricity variation for Solution 2 of Table 10

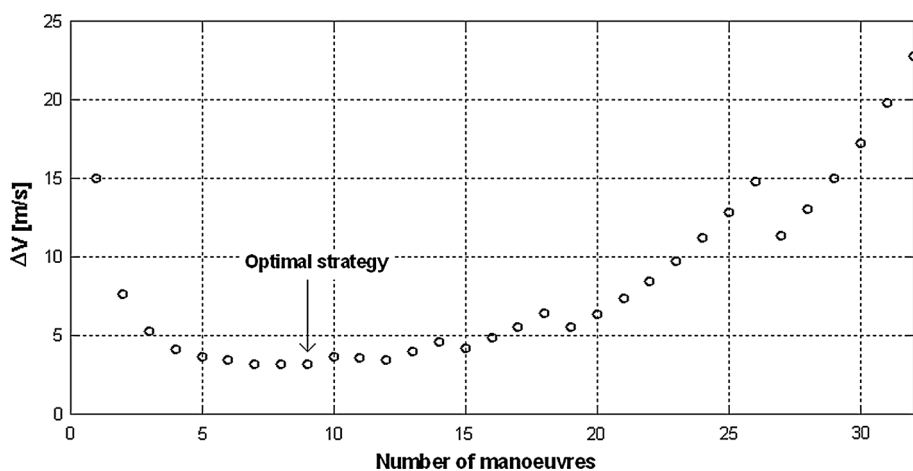


Fig. 6 ΔV as a function of the number of manoeuvres for Solution 2

5.3 Titan

Finally, PSSOs around Titan have been analysed. In particular, due to the long duration of the nodal day, only PSSO solutions with m from 1 to 4 have been taken into consideration. This way, limited revisit times have been gained. Moreover, in order to limit the drag atmospheric effects, altitudes $>1,330$ km have been taken into account. Table 11 shows the selected solutions.

Table 11 PSSO solutions around Titan

h (km)	i (°)	T _n (h)	R	m	S _m (km)
1,465.93	101.47	4.7316	81	1	199.74
1,499.54	101.24	4.7907	80	1	202.24
1,568.90	100.79	4.9136	78	1	207.43
1,353.55	102.29	4.5356	169	2	95.73
1,317.80	102.56	4.4738	257	3	62.95
1,327.93	102.48	4.4913	256	3	63.20
1,348.39	102.32	4.5267	254	3	63.70
1,422.18	101.78	4.6550	247	3	65.50
1,454.88	101.55	4.7122	244	3	66.31
1,488.26	101.32	4.7709	241	3	67.13
1,592.68	100.64	4.9559	232	3	69.74
1,300.23	102.70	4.4436	345	4	46.90
1,345.82	102.34	4.5222	339	4	47.73
1,376.97	102.11	4.5762	335	4	48.30
1,392.78	101.99	4.6037	333	4	48.59
1,408.75	101.88	4.6315	331	4	48.88
1,424.88	101.76	4.6597	329	4	49.18
1,491.07	101.30	4.7758	321	4	50.40
1,508.05	101.18	4.8057	319	4	50.72
1,560.07	100.85	4.8979	313	4	51.69

The obtained orbit inclinations allow a quasi-complete latitudinal coverage of the moon. Moreover, similar to the case of Callisto, very small distances between adjacent ground track have been gained (the maximum value of S_m is 207.43 km) and, therefore, a limited swath for the on board instrument will be required to achieve complete longitudinal coverage.

Finally, the analysis of the perturbative effects has highlighted the feasibility of exploiting these solutions without introducing corrective manoeuvres, except small semi-major variations devoted to compensate the drag atmospheric effects.

6 Conclusions

The concepts of PSSO and PMSSO have been applied to trajectories for the observation of the planets of the Solar System and of their principal moons.

For Mercury and Venus it has not been possible to obtain solutions because of limitations linked respectively to the planetary orbit eccentricity and gravitational field. For Saturn, Uranus and Neptune the employment of these kinds of orbits would not result optimal due to the long distance from the Sun, which implies very low values of solar irradiance. On the contrary, useful solutions for the investigation of planetary and atmospheric parameters have been found around both Mars and Jupiter.

Interesting applications may also be carried out around the natural satellites of Jupiter and Saturn. Since in these cases the hypothesis of J_2 predominant is not verified, the analysis has been numerically conducted. The results have highlighted the possibility of

obtaining PSSOs around Callisto and Titan, and both PSSOs and PMSSOs around Europa. In particular, in order to limit the third-body effects, the solutions around Europa have to be characterized by orbit inclinations lower than 45° . Short revisit times and high temporal samplings, not requiring corrective manoeuvres, have been found. The solutions around Callisto have shown good stability. In fact, for life-times up to 4 years, corrective manoeuvres are not required while for longer missions the needed energy remains limited. Finally, also the solutions around Titan, which are characterized by a higher altitude to limit the effects of atmospheric drag, have demonstrated good stability, thus offering the possibility of performing cyclic observations of this satellite.

References

- J.D. Anderson, R.A. Jacobson, E.L. Lau, W.B. Moore, G. Schubert, Io's gravity field and interior structure. *J. Geophys. Res.* **106**(E12), 32963–32969 (2001a)
- J.D. Anderson, R.A. Jacobson, T.P. Mc Elrath, W.B. Moore, G. Schubert, P.C. Thomas, Shape, mean radius, gravity field, and interior structure of Callisto. *Icarus* **153**(1), 157–161 (2001b)
- J.D. Anderson, E.L. Lau, W.L. Sjogren, Gravitational constraints on the internal structure of Ganymede. *Nature* **384**(6609), 541–543 (1996)
- J.D. Anderson, G. Schubert, R.A. Jacobson, E.L. Lau, W.B. Moore, W.L. Sjogren, Europa's differentiated internal structure: inferences from four Galileo encounters. *Science* **281**(5385), 2019–2022 (1998)
- P. Anderson, M. Macdonald, C. Yen, Novel orbits of mercury, venus and mars enabled using low-thrust propulsion. *Acta Astronaut.* (2013). doi:[10.1016/j.actaastro.2013.08.018](https://doi.org/10.1016/j.actaastro.2013.08.018)
- M. Aorpimai, P.L. Palmer, Analysis of frozen conditions and optimal frozen orbit insertion. *J. Guid. Control Dyn.* **26**(5), 786–793 (2003)
- M. Capderou, F. Forget, Optimal orbits for Mars atmosphere remote sensing. *Planet. Space Sci.* **52**, 789–798 (2004)
- C. Circi, E. Ortore, F. Bunkheila, C. Olivieri, Elliptical multi-sun-synchronous orbits for Mars exploration. *Celest. Mech. Dyn. Astron.* **114**(3), 215–227 (2012)
- S.L. Coffey, A. Deprit, B.L. Miller, The critical inclination in artificial satellite theory. *Celest. Mech. Dyn. Astron.* **39**, 365–406 (1986)
- S.L. Coffey, A. Deprit, E. Deprit, Frozen orbits for satellites close to an earth-like planet. *Celest. Mech. Dyn. Astron.* **59**, 37–72 (1994)
- L. Iess, N.J. Rappaport, R.A. Jacobson, P. Racioppa, D.J. Stevenson, P. Tortora, J.W. Armstrong, S.W. Asmar, Gravity field, shape, and moment of inertia of titan. *Science* **327**(5971), 1367–1369 (2010)
- A.S. Konopliv, W.B. Banerdt, W.L. Sjogren, Venus gravity: 180th degree and order model. *Icarus* **139**(1), 3–18 (1999)
- M. Lara, R. Russell, Computation of a science orbit about Europa. *J. Guid. Control Dyn.* **30**(1), 259–263 (2007)
- X. Liu, H. Baoyin, X. Ma, Five special types of orbits around Mars. *J. Guid. Control Dyn.* **33**(4), 1294–1301 (2010)
- X. Liu, H. Baoyin, X. Ma, Analytical investigations of quasi-circular frozen orbits in the Martian gravity field. *Celest. Mech. Dyn. Astron.* **109**, 303–320 (2011a)
- X. Liu, H. Baoyin, X. Ma, Extension of the critical inclination. *Astrophys. Space Sci.* **334**, 115–124 (2011b)
- X. Liu, H. Baoyin, X. Ma, Periodic orbits around aerostationary points in the Martian gravity field. *Res. Astron. Astrophys.* **12**(5), 551–562 (2012)
- E. Ortore, C. Olivieri, A small satellite constellation for continuous coverage of mid-low earth latitudes. *J. Astronaut. Sci.* **56**(2), 185–198 (2008)
- E. Ortore, C. Olivieri, F. Bunkheila, Satellite constellations in inclined multi-stationary orbits. *Proc. Inst. Mech. Eng. Part G J. Aerosp. Eng.* **225**(9), 1050–1060 (2011)
- E. Ortore, C. Circi, F. Bunkheila, C. Olivieri, Earth and mars observation using periodic orbits. *Adv. Space Res.* **49**(1), 185–195 (2012)
- E. Ortore, C. Circi, F. Bunkheila, C. Olivieri, Retrieval of aerosol properties by using low earth orbit. *Aerosp. Sci. Technol.* **30**(1), 333–338 (2013)
- I. Wytrzyszczak, Stationary orbits around the earth and mars. *Artif. Satell.* **33**(1), 11–23 (1998)